Optimal Design of a Molten Salt Thermal Storage Tank for Parabolic Trough Solar Power Plants

R. Gabbrielli
Dipartimento di Energetica,
Università di Pisa,
via Diotisalvi 2, Pisa 56126, Italy
e-mail: r.gabbrielli@ing.unipi.it

C. Zamparelli
ENEL GEM,
Area Tecnica Ricerca,
Via A. Pisano 120, 56100 Pisa, Italy
e-mail: carlo.zamparelli@enel.it

This paper presents an optimal design procedure for internally insulated, carbon steel, molten salt thermal storage tanks for parabolic trough solar power plants. The exact size of the vessel and insulation layers and the shape of the roof are optimized by minimizing the total investment cost of the storage system under three technical constraints: remaining within the maximum allowable values of both temperature and stress in the steel structure, and avoiding excessive cooling and consequent solidification of the molten salt during long periods of no solar input. The thermal, mechanical and economic aspects have been integrated into an iterative step-by-step optimization procedure, which is shown to be effective through application to the case study of a 600 MW h thermal storage system. The optimal design turns out to be an internally insulated, carbon steel storage tank characterized by a maximum allowable height of 11 m and a diameter of 22.4 m. The total investment cost is about 20% lower than that of a corresponding AISI 321H stainless steel storage tank without internal protection or insulation.
[DOI: 10.1115/1.3197585]

Keywords: parabolic trough, molten salt, optimal design, thermal storage tank, solar power plant

1 Introduction

Solar thermal power plants are attractive solutions for generating electricity from renewable energy sources. Large-scale applications include the implementation of parabolic trough technology, linear Fresnel reflector technologies, single tower systems, distributed tower systems, and updraft towers [1,2]. Nowadays, parabolic trough technology is the most proven and cost-efficient, large-scale solar power technology available, thanks to the experience acquired at several commercial solar electric generating systems (SEGS) in California.

In parabolic trough systems, direct solar radiation is converted into thermal power used by heating a suitable medium. Two configurations are available: direct steam generation (DSG) and fluid-based thermal storage systems. In DSG systems, the medium is high-pressure water that is superheated as it passes through the absorber pipes of parabolic trough collectors in the solar field. The steam directly feeds a steam turbine for power generation, as in the common Rankine cycle [3–8]. In this way, the direct solar radiation is converted into electric power in real time.

The second option is characterized by the presence of a thermal fluid that crosses solar collectors and is consequently heated. This fluid can be used either as a storage medium itself, and is consequently accumulated inside suitable storage tank, or as a thermal vector to transfer the energy to a different storage medium. The high-temperature storage fluid is subsequently cooled in a heat exchanger to produce high-pressure, superheated steam for power generation. The power plant can be either a stand-alone steam cycle, as in DSG systems, or integrated solar combined cycle systems (ISCCSs), where the solar-derived steam is mixed with that produced in a standard gas turbine combined cycle [9].

The presence of thermal storage implies the following operational advantages over DSG: (i) the steam power plant can operate under constant conditions with higher thermal efficiency, thereby mitigating any changes in direct solar radiation; (ii) it is possible to convert thermal power into electrical when the market price of electricity is highest, thereby affording the greatest economic return; (iii) storage makes it possible to meet peaks in electricity demand. The main options for actual utilization of thermal energy storage are [10] (1) buffering during transitory weather conditions, (2) dispatchability or time shifting, (3) increased annual capacity factor, and (4) more even distribution of electricity production.

Several storage systems for parabolic trough solar power plants have been proposed in the literature [10]: sensible heat storage both in solid media [11] and in liquid media [12,13]; latent heat storage, whereby the thermal medium undergoes a phase change [14]; and chemical storage, in which the solar energy is stored and extracted by reversing the direction of endothermal reactions, respectively, from reactants to products and vice versa.

Regarding sensible heat storage in the liquid phase, which can be considered the simplest and cheapest method, it is possible to adopt one- or two-tank configurations. In the former type, thermal stratification is present within the tank (thermocline tank), whereby the hot liquid accumulates at the top level and the cold is stratified at the bottom [15,16]. In the other configuration, the hot and cold fluids are stored separately in two tanks. The hot storage fluid is conveyed from the high-temperature tank to the "cold" tank after cooling during steam generation. Although storage volume and costs are clearly lower in single-tank systems, it is more difficult to separate the hot and cold thermal fluids due to the density difference between the cold layer at the bottom and the hot one at the top [10]. The main advantage of two-tank configurations is that the cold and hot thermal fluid are stored separately, and the system's operation is consequently simpler. On the contrary, this configuration is plainly more expensive because of the need for the second tank. Several thermal storage fluids have been proposed for parabolic trough solar power plants [13]. From the perspectives of economy and safety, molten salts are considered

Contributed by the Solar Energy Engineering Division of ASME for publication in the JOURNAL OF SOLAR ENERGY ENGINEERING. Manuscript received February 22, 2007; final manuscript received November 27, 2007; published online September 17, 2009. Review conducted by Rainer Tamme.

Table 1 Characteristics of molten salt thermal fluid

$NaNO_3$=60	Composition,
KNO_3=40	%mass content
1740.2	Density, kg/m^3 (550°C)
1905.5	Density, kg/m^3 (290°C)
1537.6	Specific heat, kJ/kg K (550°C)
1492.9	Specific heat, J/kg K (290°C)
0.5475	Conductivity, W/m K (550°C)
0.4981	Conductivity, W/m K (290°C)
600	Max allowable temperature, °C
238	Min allowable temperature, °C
0.5	Cost, €/kg

the most promising, as they are less expensive and more environmentally "friendly" than mineral oils. Moreover, they can be heated up to 600°C, whereas the highest allowable temperature for mineral oils is about 300°C. This enables achieving overall greater thermal efficiency of the solar power plant.

In a two-tank configuration of a parabolic trough solar power plant with sensible heat thermal storage, the storage tanks are amongst the most critical components. Economic and safety aspects require accurate design. In this paper, a structured optimization procedure, wherein thermal, structural, and economic aspects are integrated together, is proposed as an effective tool to support the design procedure of molten salt, cylindrical storage tanks. The paper is divided into the following sections. First, the data, constraints and hypotheses adopted in the tank design are set forth. Then, the following iterative steps for optimizing the tank design are described: (i) defining the structural characteristics of the storage tank and its constituent elements, (ii) calculating the thermal profiles within the tank's interior as well as the unsteady analysis of molten salt cooling, (iii) evaluating the stresses in the vessel plates via the finite element method (FEM) and selecting the most suitable shape for the roof, and (iv) evaluating the total investment cost (TIC). Lastly, some closing observations and remarks are advanced in the conclusions.

2 Data, Constraints, and Main Assumptions for Tank Design

The parabolic trough solar thermal power plant in question is located in southern Italy, where the average direct normal irradiance is about 1900 kW h/m^2 year. The plant, whose useful solar collection surface is about 190,000 m^2, is made up of the following main components: (i) parabolic trough solar field, where the cold molten salt—a mixture of potassium and sodium nitrates (Table 1)—is heated to 550°C; (ii) high-temperature atmospheric storage tank, where the hot molten salt is collected downstream from the solar field; (iii) molten salt-water/steam heat exchanger, where the thermal fluid is cooled to 290°C in the process of superheating the steam (which is then integrated in a gas turbine combined cycle with nominal power of about 380 MWe); and (iv) low-temperature storage tank, where the cold thermal fluid is collected downstream from the heat exchanger.

During the design stage of the storage system, a number of constraints must be respected. In order to ensure that the solar plant, whose nominal thermal power is 60 MW_{th}, functions continuously over a period of 10 h, the thermal capacity of the storage system must be 600 MWh, which correspond to about 5500 t of molten salts. Each tank must be able to store the entire supply of thermal fluid, as such working conditions could occur at start-up and draining of the solar power plant, when all the thermal fluid is amassed in a single tank.

In order to enable high flexibility in operations, the roles of the high- and low-temperature tanks must be interchangeable. Indeed, in the event of shell failure, it could, for safety reasons, become necessary to quickly discharge the hot tank and fill the cold one, without allowing the hot molten salts to cool through the heat exchanger. Hence, in spite of the increased storage costs, from the point of view of resistance, the low-temperature tank design must be allow for its operating at the maximum permissible temperature. In order to reduce the cost of the storage system, a conventional carbon steel with maximum allowable working temperature of 315°C has been chosen for fashioning the vessel.

The molten salt thermal fluid from each tank is delivered by a long-shaft centrifugal vertical pump, whose impeller is submerged and located just above the bottom of the tank and whose motor must be mounted above the tank roof with suitable piping for delivery. Molten salt delivery from the lateral surface of the tank has not been envisaged, as this would involve the introduction of critical points in the cylindrical shell, with possible reduction in the structural strength—a situation best avoided. Moreover, the possibility of adopting a fully submerged pump has likewise been disregarded due to the corrosive conditions within high-temperature molten salts. After an exhaustive review of the pumps available on the market, the maximum allowable shaft length has been fixed at 12 m, which introduces a design constraint for the maximum tank height, H.

Lastly, from the structural point of view, during the design stage of the tank, the possibility of overpressure and vacuum-load conditions must also be taken into account. These two conditions could occur, respectively, when a heat exchanger pipe failure allows high-pressure steam to enter the tank, or when the tank breathing system fails in the closed position and the hot molten salts cool suddenly.

3 Iterative Procedure for Optimal Design of the Storage Tank

The iterative optimising procedure for designing the storage tank is summarized in Fig. 1. After deciding upon the type of construction best able to guarantee efficient, safe storage of the high-temperature molten salt mixture, the salt storage chamber is provisionally assigned a height and diameter. Then, the thickness of each protective layer, as well as the choice of thermal insulating materials, is defined.

At this point, it is possible to evaluate the temperature profile within the storage tank and analyze the unsteady cooling of the molten salts due to heat loss to the environment. If the metal temperature is higher than the admissible value, or the thermal fluid cooling is excessive, the thickness of insulating protective layers must be adjusted accordingly. Then, the thickness of each shell plate is defined, and respect for the maximum allowable plate stress is checked using FEM and the metal temperature data. If the limits are exceeded, the plates are redesigned. The best roof shape to withstand failure conditions of overpressure and vacuum can also be assessed via the FEM analysis.

Lastly, the total cost of the storage system is calculated. If the defined configuration minimizes cost, the optimal design procedure ends; otherwise, it will be necessary either to adopt different thicknesses of the insulating materials or modify the chamber size, and then repeat the whole design procedure.

4 Molten Salt Storage-Tank Construction

The cylindrical storage-tank vessel, which is not in direct contact with the high-temperature fluid, is made of SA-516 Gr-70 carbon steel. Its internal surface is protected by a layer of insulating firebricks, characterized by very high porosity and low density. The firebricks are protected against contact with the molten

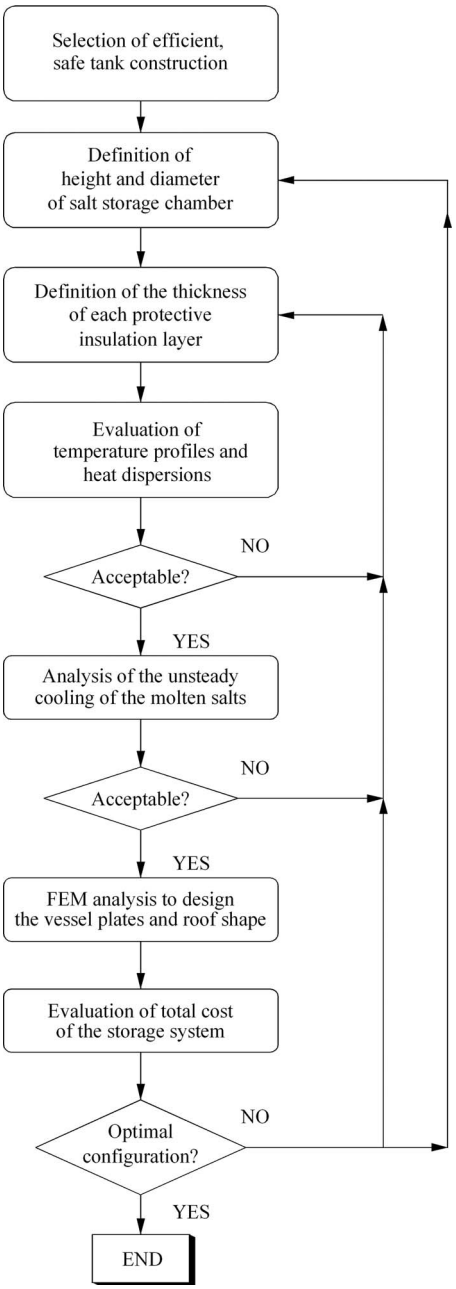

Fig. 1 Optimization procedure for design of the storage system

salts by a flexible AISI 321H stainless steel liner (Fig. 2), which is corrugated in both the horizontal and longitudinal directions. These corrugations ensure that the liner can safely withstand the thermal strains. The stainless steel selected for the liner seems to possess the necessary resistance to the corrosive action of the high-temperature molten salts with which it will be in contact. Thanks to the firebrick layer, the hydrostatic pressure due to the molten salt head is transferred directly to the steel vessel through the flexible liner and the firebrick layer. In order to ensure good contact between firebricks and vessel, a thin layer of ceramic fiber insulating material is positioned behind the firebricks. Resistance to thermal strains and stability of the firebrick column are ensured by mounting the firebricks on brackets welded to the steel vessel (Fig. 3).

The external surface of the shell is protected by a coat of ceramic fiber insulation, which is, in turn, covered by a thin aluminium sheet. The bottom of the steel vessel is protected from contact with the molten salts by the flexible liner and a separate insulating layer of firebricks (Fig. 4).

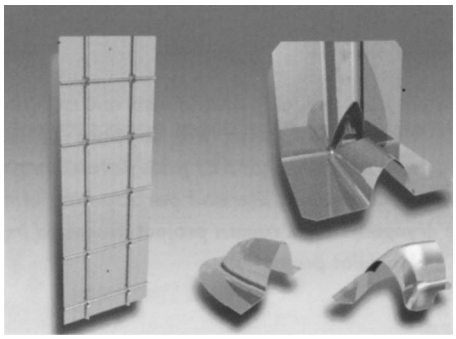

Fig. 2 Flexible protective liner made of AISI 321H stainless steel

A vessel configuration in which the flexible protective liner and insulating firebricks are not used and the molten salts would consequently be in direct contact with the steel vessel has been discounted due to the high associated cost.

The tank foundation is made up of several protective layers (Fig. 4): fine sand, insulating firebricks, foamglas®, cooled reinforced concrete, poor concrete slab, and foundation piles. Foamglas® possesses very attractive properties in terms of thermal insulation and compressive strength. In order to ensure that the working temperature reached in the concrete remains below the maximum allowable value of 100°C, horizontal tubes for cooling water are embedded within the foundation.

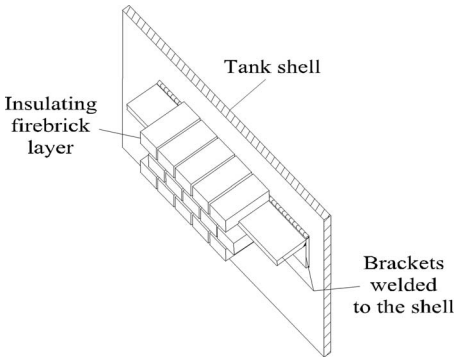

Fig. 3 Insulating firebrick layer, which protects the tank shell

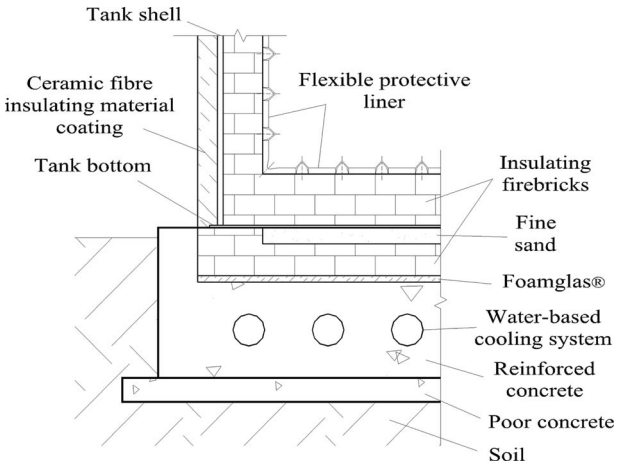

Fig. 4 Scheme of the storage-tank foundation construction

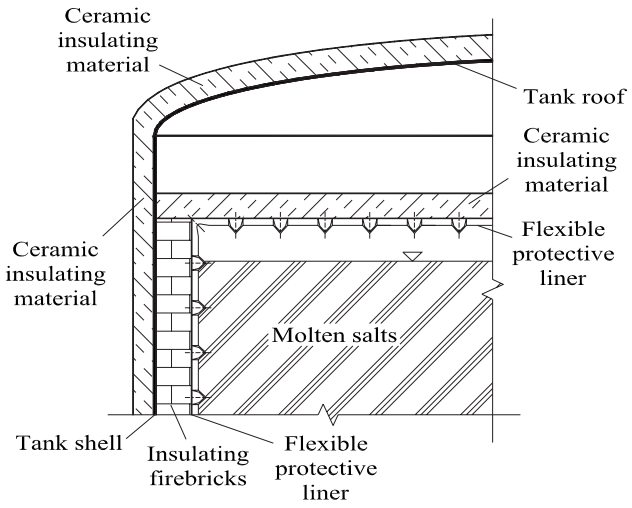

Fig. 5 Scheme of the storage-tank roof construction

The tank roof (Fig. 5) is made up of a fixed ellipsoid-shaped sheet. A floating configuration and column-sustained type roof have both been discounted due to the technical problems stemming from direct contact with the high-temperature molten salts, in the case of the former, and potential settling of the bottom firebrick layer, in the latter. The flexible stainless steel liner continues above the molten salts, so that it forms a closed cylindrical storage chamber. The upper surface of the liner is coated with ceramic fiber insulating material and is hung from the roof, whose external surface is moreover protected by another layer of ceramic fibre insulation, which further reduces heat loss to the environment.

Clearly, the temperature of the molten salt must not fall below the minimum allowable value, which corresponds to the initial crystallization temperature of the molten salts. Therefore, in order to ensure that crystallization does not initiate during plant stoppages or periods without direct solar irradiation, the tanks must be fitted with a suitable heating system.

5 Design of the Molten Salt Storage Tank

5.1 Evaluating Temperature Profiles and Heat Losses. The tank temperature profiles and the loss of heat from the tank to the environment have been evaluated using the thermal scheme shown in Fig. 6. As a first approximation, the thermal resistance to heat flux to the external environment through the tank's lateral surfaces, roof, and foundation can be considered in parallel. The cooling system, which maintains the concrete temperature (T_{conc}) at 90°C, divides the thermal resistance of the foundation into two parts, which can be considered to be in series.

The overall heat loss from the storage tank, i.e., from the lateral surface, foundation, and roof, decreases as a function of the tank height, H, as reported in Fig. 7 for a representative insulation configuration. H appears to be the most relevant variable with regard to the heat loss. Figure 7 (as well as the following) shows that the range of values of H exceeds the constraint imposed by the maximum pump shaft length and thereby provides a broad overview of possible design results under ideal conditions.

The temperatures of the tank shell, roof, and bottom increase with the thicknesses of the insulating coat outside the tank and

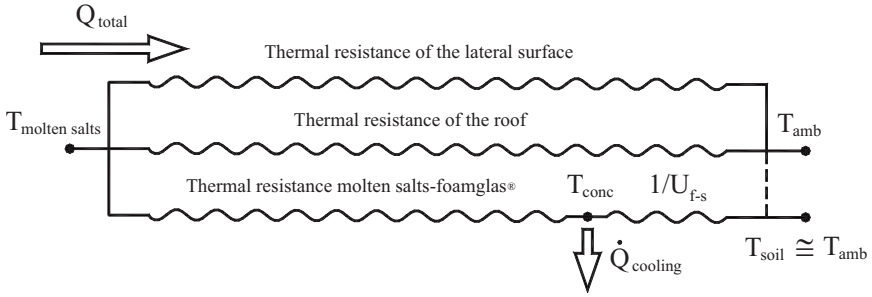

Fig. 6 Scheme of the thermal losses to the environment

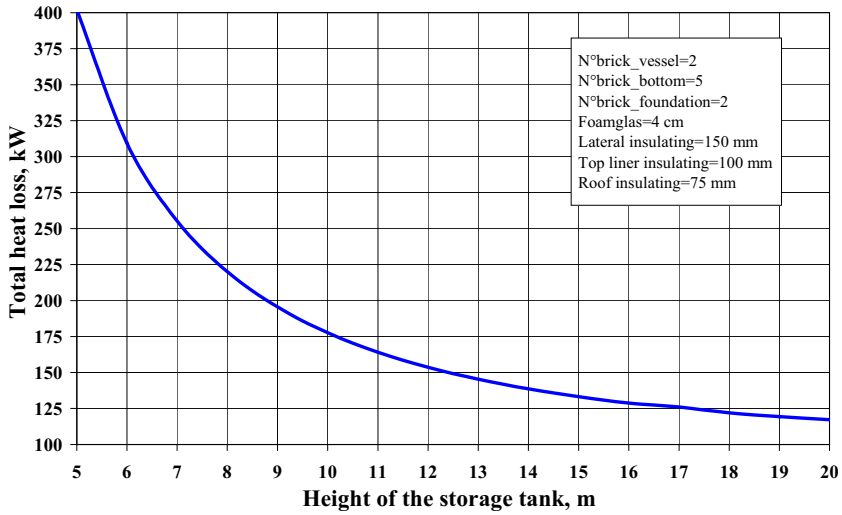

Fig. 7 Total heat loss from the storage tank as a function of tank height for a particular insulation configuration

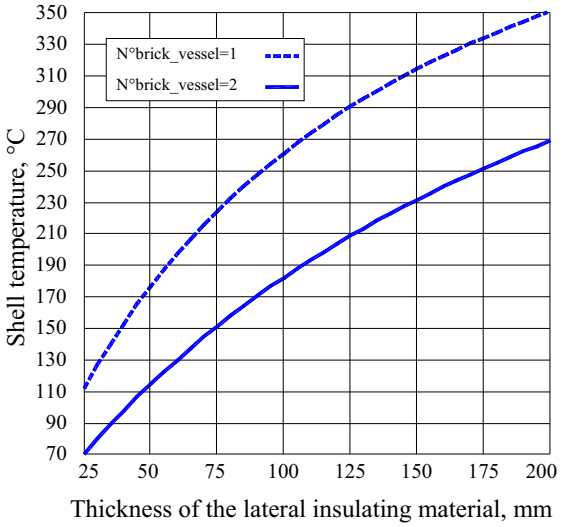

Fig. 8 Shell temperature as a function of the lateral insulating material

decrease as the insulation within the tank is increased (Figs. 8 and 9 and Table 2). These figures clearly evidence the feasible range of the protective insulating coatings, which ensure that the maximum allowable temperature for the steel vessel is not exceeded. It is interesting to note that the thermal analysis showed that the temperature of the steel tank is practically independent of the tank height (not reported in Fig. 8).

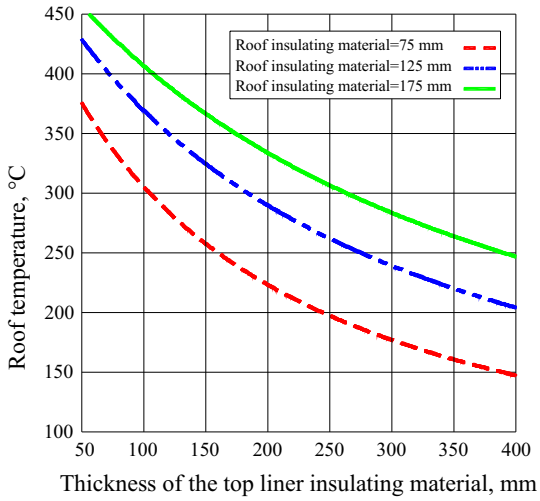

Fig. 9 Roof temperature as a function of the top liner insulating material

Table 2 Tank bottom temperature as a function of foundation insulating characteristics

No. of brick bottom	No. of brick foundation	Foamglas® thickness (cm)	Temperature of tank bottom (°C)
2	2	4	401
2	5	4	457
5	2	4	299
5	5	4	372
2	2	12	444
2	5	12	476
5	2	12	353
5	5	12	401

5.2 Analysis of the Unsteady Cooling of the Molten Salts. During periods of no solar input, the thermal fluid inside the storage tanks cools due to heat loss to the environment. Any technical solutions for storage can only be considered feasible if the temperature decrease of the molten salt is so limited that solidification, which would cause enormous operational difficulties, does not occur.

Despite the presence of heaters incorporated into the tank bottom, it is important to verify the unsteady thermal behavior of the molten salts. As a first approximation, we can neglect the dependence of the physical parameters on temperature, in which case the differential equation for the thermal balance of the molten salt is the following:

$$m_{\text{salt}} \cdot Cp_{\text{salt}} \cdot \frac{dT_{\text{salt}}(t)}{dt} = \frac{T_{\text{salt}}(t) - T_{\text{amb}}}{R_{\text{tot\_lat}}} + \frac{T_{\text{salt}}(t) - T_{\text{amb}}}{R_{\text{tot\_roof}}} + \frac{T_{\text{salt}}(t) - T_{\text{conc}}}{R_{\text{salt-foam}}} \tag{1}$$

By solving Eq. (1), we obtain the analytical expression for the molten salt temperature as a function of time:

$$T_{\text{salt}}(t) = \frac{R_{\text{tot}}}{R^*_{\text{tot}}} \cdot T_{\text{amb}} + \frac{R_{\text{tot}}}{R_{\text{salt-foam}}} T_{\text{conc}} + \left[T_{\text{salt=0}} - \left(\frac{R_{\text{tot}}}{R^*_{\text{tot}}} \cdot T_{\text{amb}} + \frac{R_{\text{tot}}}{R_{\text{salt-foam}}} \cdot T_{\text{conc}} \right) \right] \times \exp\left(- \frac{1}{R_{\text{tot}} \cdot m_{\text{salt}} \cdot Cp_{\text{salt}}} \cdot t \right) \tag{2}$$

where

$$R_{\text{tot}} = \left(\frac{1}{R_{\text{tot\_lat}}} + \frac{1}{R_{\text{tot\_roof}}} + \frac{1}{R_{\text{salt-foam}}} \right)^{-1}$$

$$R^*_{\text{tot}} = \left(\frac{1}{R_{\text{tot\_lat}}} + \frac{1}{R_{\text{tot\_roof}}} \right)^{-1}$$

Figure 10 represents the temperature dependence for both the hot and cold storage tanks during any given day for a rather general intermediate insulation configuration for varying quantities of stored molten salts. Even when the stored mass of molten salts is low, the overall insulation of the storage tank ensures acceptably limited cooling of the molten salts.

5.3 Stress Analysis of the Tank and Parametric Study of the Roof Shape. Once the thickness of the shell plates is fixed, a stress analysis, integrated into the optimal design procedure, can be conducted via FEM, using the SAP2000 software (rel. 8.2.3). The model is composed of shell elements with four nodes. As it had been verified numerically that contact friction force between the tank bottom and the foundation is unable to avoid sliding of the tank bottom during heating at start-up, the nodes of the shell bottom have been restrained with simple sliding bearings. In the numerical model under normal working conditions, the external loads are weight, hydrostatic head of the fluid, wind, snow, and temperature field, which is known from the foregoing analysis. The allowable stress in the carbon steel of the vessel obviously depends on the actual value of the temperature of the metal, which is calculated during the previous step of the design procedure.

The roof shape heavily influences its capacity to withstand overpressure and vacuum failure conditions. In the design procedure, it has been assumed that such loads cannot be sustained by the flexible liner due to its low thickness and high flexibility. Hence, the liner has been designed with a number of holes in its top surface to avoid failure due to overpressure and/or vacuum. The shell and roof, which are welded together, must be designed carefully so that they can safely withstand overpressure and vacuum.

If a spherical cap is used, the stress at the joint between roof

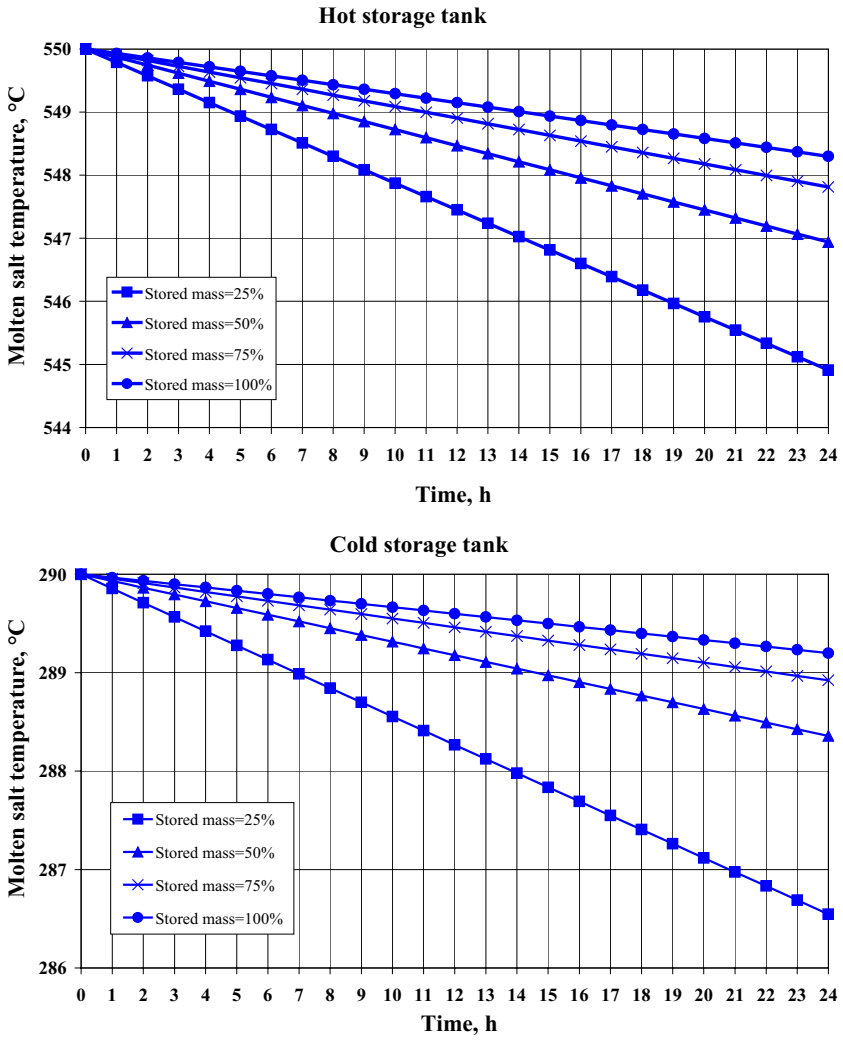

Fig. 10 Unsteady thermal behavior of the storage tanks

and shell often exceed the allowable value, even with a rather low overpressure of 10 kPa g. A storage tank with an ellipsoidal roof can withstand higher overpressures. Figure 11 shows the results for a specific ellipsoid roof configuration. The maximum allowable overpressure grows with increasing rise of the roof (Fig. 12) because the radius of curvature at the cylindrical shell-roof joint grows correspondingly. The use of a perfectly hemispherical roof, which would result in the lowest stress reach values, is not fea-

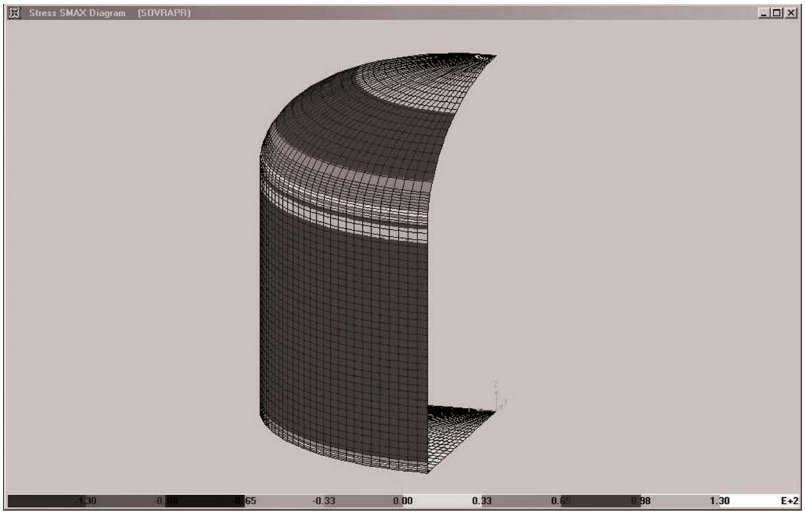

Fig. 11 Maximum principal stresses with ellipsoid shape, rise=5.5 m, thickness=12.5 mm, and overpressure=120 kPa g

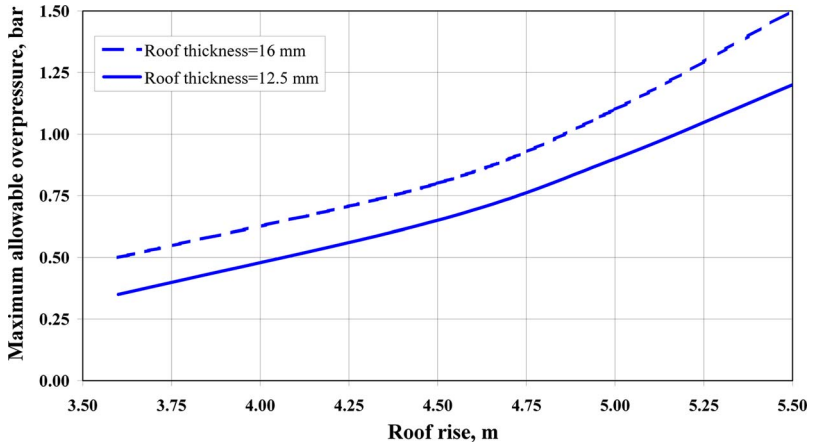

Fig. 12 Maximum allowable overpressure of the storage tank with ellipsoidal roof

sible due to the consequently excessive rise, which would cause problems in pump installation.

The cylindrical shell-bottom joint is not limited by the same critical factor described above for the shell-roof joint, thanks to the presence of suitable anchorage at the bottom plates' borders, which enables it to resist uplift due to internal overpressures, as suggested by technical standards. In such a configuration, the large width of the lowest plates of the shell and the anchoring to the tank foundation ensure that resulting stresses remain below the limit value.

With regard to the vacuum load, the cylindrical shape's resistance to buckling is a critical factor. As reported in Fig. 13, without ring stiffeners, the storage tank can withstand only very low vacuum levels, despite a very large thickness. Hence, based on the results described above, the presence of some reliable passive protection system, such as rupture disks, is unavoidable to ensure storage-tank safety.

5.4 Economic Analysis. The final step in the optimal design procedure is economic analysis. The TIC encompasses the cost for construction and installation of two identical storage tanks, the purchase of molten salt (0.5 €/kg) and the overall cost of actual

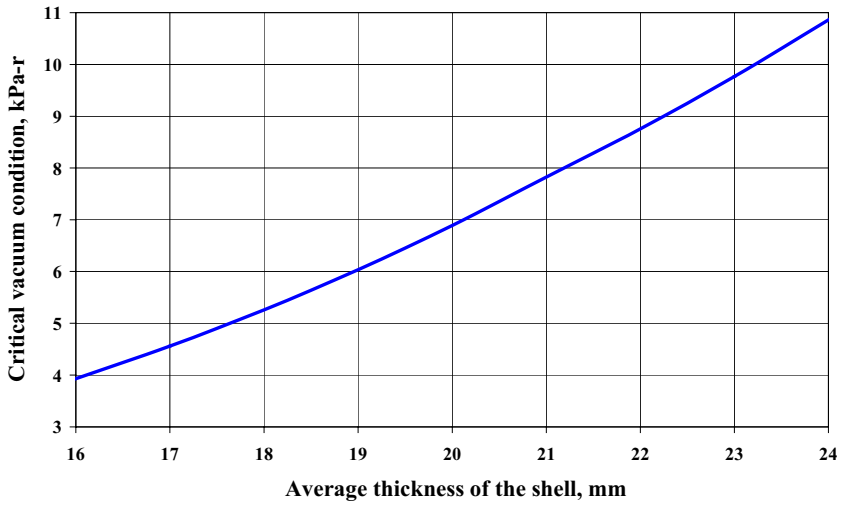

Fig. 13 Critical vacuum condition vs average shell thickness

Table 3 Specific costs of storage system components

	SA-516 Gr-70 (€/t)	Insulating firebricks (€/piece)	Flexible liner (€/kg)	Ceramic fibre insulating material (25 mm thick) (€/m^2)	Foamglas®, (40 mm-thick slab) (€/m^2)	Reinforced concrete (€/m^3)	Piles (€/piece)
Specific purchase cost	701	0.465	1.5	7.918	14.5	150	1000
Installation coefficient	3	1.5	10	1.5	1.5	1	1

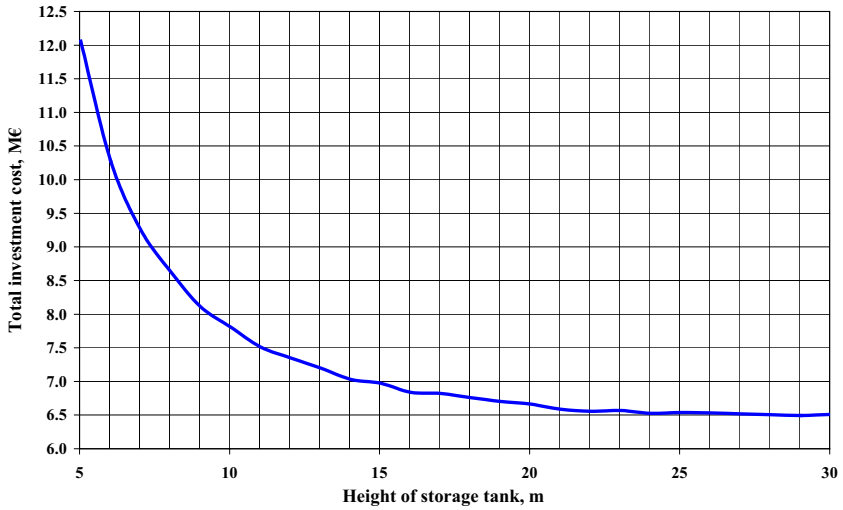

Fig. 14 Overall investment cost of the storage system as a function of *H*

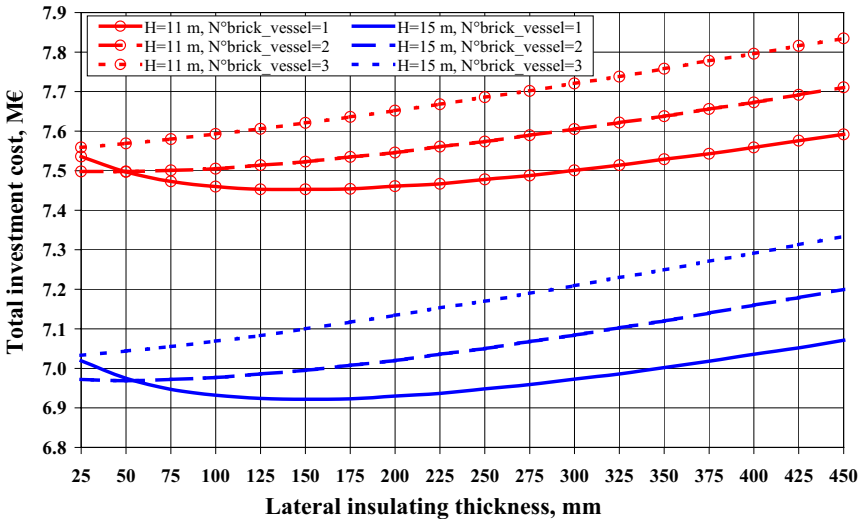

Fig. 15 Total investment cost of the storage system as a function of the lateral insulating material for some values of *H* and number of lateral insulating firebricks

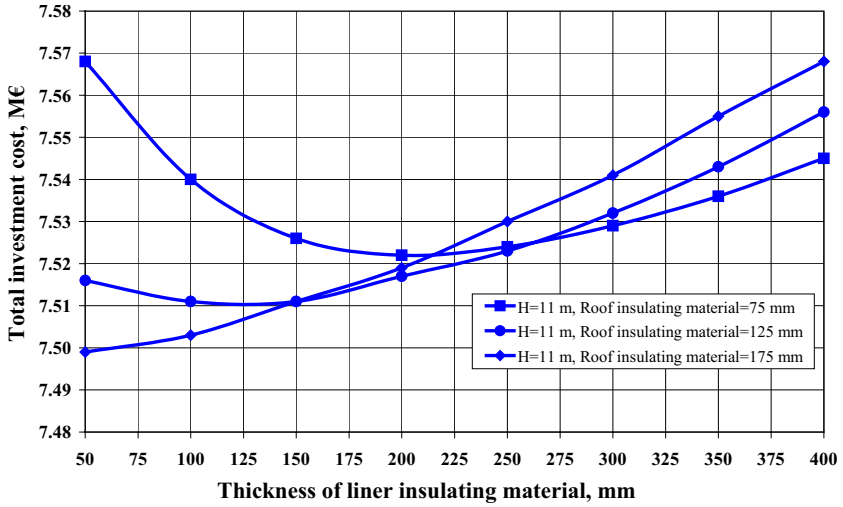

Fig. 16 Total investment cost of the storage system as a function of the liner insulating material for some values of the roof insulating material

operations associated with heat loss to the environment. For each storage-tank component, the construction and installation cost has been evaluated using specific purchase cost data (Table 3), the values of which have been multiplied by both the overall material quantity and a suitable installation coefficient (Table 3). The foundation piles have been sized in consideration of the overall weight of the storage system. In particular, it has been assumed that each pile must be able to sustain about 1 t.

The thermal energy, which is available in the storage tank in the form of sensible heat and leaks into the environment, obviously cannot be converted into electric energy via steam production in the heat exchanger. This involves a substantial operations cost, whose overall actualised value ($C_{\text{heat loss}}$) can be calculated as follows:

$$C_{\text{heat loss}} = (1 - t_{\text{ax}}) \cdot F \cdot \sum_{k=1}^{D_{\text{GC}}} \left[\frac{1}{(1+i)^k} \cdot \left[C_{\text{GC}} \cdot (1 + r_{\text{GC}})^k + C_e \cdot (1+r)^k \right] \cdot \left(\sum_{s=1}^{12} \dot{Q}_{\text{total-}s} \cdot \eta_s \cdot h_s \right) \right] + \sum_{k=D_{\text{GC}}+1}^{N} \left[\frac{(1+r)^k}{(1+i)^k} \cdot C_e \cdot \sum_{s=1}^{12} \dot{Q}_{\text{total-}s} \cdot \eta_s \cdot h_s \right] \quad (3)$$

where $\dot{Q}_{\text{total-}s} \cdot \eta_s$ is the electric power, which could be produced with $\dot{Q}_{\text{total-}s}$, and $\dot{Q}_{\text{total-}s} \cdot \eta_s \cdot h_s$ is the electricity which could be produced during any given month, s. In Eq. (3), the actual annual outcome for the unsold electricity over any given year obviously depends on the market price of electricity. During the first 12 years of the system's operational lifetime, it is possible to obtain green certificates for renewable energy. $\dot{Q}_{\text{total-}s}$ depends on the average ambient temperature, which clearly varies over the course of a year. Hence, in order to calculate the average temperature, we have utilized experimentally determined ambient temperature values for the particular Italian site where the solar power plant is to be located. The efficiency, η_s, of conversion of the solar-derived thermal energy into electricity depends on the overall solar power actually integrated within the combined cycle and, accordingly, on the monthly solar load over the course of the year, whose annual average value turns out to be about 41%.

For all insulation configurations, the TIC decreases monotonically with H (Fig. 14). Hence, the optimal storage-tank size corresponds to the maximum allowable height, which is dictated by the shaft length of the vertical pump.

With regard to the cost contributions of the lateral insulating material thickness and No. of brick_vessel, the TIC is minimized when these values are, respectively, 125 mm and 1 (Fig. 15). These values are practically independent of H. The dependence of the TIC on the roof insulating layers is very low (Fig. 16). Hence, adjusting the actual thickness of these layers is not particularly important in terms of cost. However, the roof insulating layers are obviously important for the temperature profile of the tank.

Table 4 summarizes the dependence of TIC on the foundation parameters. Once H has been fixed, the TIC varies very little. Hence, the foundation insulation is of practical importance only with regard to the temperature of the tank bottom.

Lastly, Table 5 presents a brief capital cost comparison between the internally insulated, carbon steel storage tank described above, and a design utilizing AISI 321H stainless steel without any internal protection. A tank with the maximum allowable height of 11 m has been used as reference. Selecting such height, it is an easy matter to mount the pump on the ellipsoidal roof of the tanks and respect the constraint imposed by the maximum shaft length. In the stainless steel storage-tank design, the molten salts are in direct contact with the vessel and, consequently, the flexible liner and internal insulating firebricks are lacking. In this comparison, the overall insulation configuration of both tank solutions has been adjusted to equal the overall heat loss to the environment. The stainless steel storage tank turns out to be about 1.650 M€ more expensive than the carbon steel one. Such difference is mostly due to the higher costs involved with acquiring the stainless steel and actually building the vessel. Indeed, adopting the AISI 321H design, the allowable stress at 550°C is about half, and the purchase price of steel about double the corresponding values for the SA-516 Gr-70 steel design. Moreover, the weight of the necessary AISI 321H plates would be about 45% greater than that of the carbon steel. Table 5 shows only those parameters revealing significant differences between the two solutions.

Table 4 Total investment cost dependence on some characteristics of the tank foundation

H (m)	No. of brick bottom	No. of brick foundation	Foamglas® thickness (cm)	Total investment cost (M€)
11	2	2	4	7.48
11	2	5	4	7.50
11	5	2	4	7.51
11	5	5	4	7.56
15	2	2	4	6.91
15	2	5	4	6.92
15	5	2	4	6.99
15	5	5	4	7.02
11	2	2	12	7.48
11	2	5	12	7.52
11	5	2	12	7.53
11	5	5	12	7.58
15	2	2	12	6.91
15	2	5	12	6.94
15	5	2	12	7.00
15	5	5	12	7.03

6 Conclusions

This paper has presented a structured approach to optimizing the design of a molten salt storage system for a parabolic trough solar power plant. The iterative step-by-step procedure reveals to be an effective tool for such end, as it ensures that both the thermal and structural aspects relevant to heat loss and external loads are effectively considered in an integrated way to obtain a feasible, optimal technical solution. The procedure has been applied to the case study of a 600 MW h thermal storage system, for which an optimal configuration is determined and described.

Table 5 Capital cost comparison between internally insulated carbon steel storage tank and AISI 321H stainless steel storage tank

	Internally insulated carbon steel storage tank	Stainless steel storage tank
Diameter (m)	22.4	22.4
H (m)	11	11
Q_{total} (kW)	187	187
Weight of steel, tons	279	410
Thickness of the lateral insulation material, mm	125	250
Roof insulating thinckness (mm)	125	200
Foamglas® thickness, mm	40	200
No. of brick_foundation	2	2
No. of brick_vessel (radially mounted)	1	0
No. of brick_bottom	5	0
TIC (M€)	7.45	9.13
Cost of steel (M€)	1.04	3.27
Cost of flexible liner (k€)	482	0

Evaluation of the temperature profile within the tank makes it possible to define the feasible domain of the design variables, such as the thickness of the insulation layers of the shell vessel.

The specific technical solutions resulting from application of the design procedure appear inexpensive, feasible, and reliable. The firebrick layers, which protect the vessel from contact with the high-temperature molten salts, make it possible to lower the temperature and adopt standard carbon steel for fashioning the vessel. However, some technical problems still remain unsolved with regard to two aspects of the storage tank's construction: mounting the flexible liner and securing it to the firebrick layer, and the tank's ability to safely withstand the contingencies of overpressure and/or vacuum. Ongoing research work is addressing these two phenomena, which shall be analyzed in detail in order to determine exact values on which to base the design of vessel safety systems. Future work on molten salt storage-tank design will also focus on evaluating the technical feasibility of adopting other types of stainless steel, such as AISI 347H.

Acknowledgment

The authors would like to thank the reviewers for their useful contributions to improving this paper.

Nomenclature

C_e = average selling price of electricity, €/kWh
C_{GC} = specific income associated with green certificates for solar-derived electricity, €/kWh
$C_{heat\ loss}$ = overall actualised value of the cost associated to heat losses, €
Cp_{salt} = specific heat of molten salts, kJ/kg °C
D_{GC} = validity period of green certificates, years
DSG = direct steam generation
F = average availability of the solar integrated combined cycle power plant
FEM = finite element method
H = height of the cylindrical vessel, m
h_s = overall hours of operations during any given month, s, h
i = discount rate
ISCCS = integrated solar combined cycle system
m_{salt} = actual stored mass of molten salts inside the storage tank, t
N = duration of the solar plant, years
No. of brick_bottom = number of firebricks protecting the tank bottom
No. of brick_foundation = number of firebricks protecting the tank foundation
No. of brick_vessel = number of lateral firebricks protecting the tank shell
$\dot{Q}_{cooling}$ = heat dispersed by the concrete foundation cooling system, kW
$\dot{Q}_{total}$ = overall heat loss from the molten salts, kW
$\dot{Q}_{total\text{-}s}$ = average heat loss during any month, s, during the tank's operational lifetime, kW
r = annual rate of increase of the price of electricity, %
r_{GC} = annual rate of increase of the price of green certificates, %
R_{tot} = overall thermal resistance between the molten salts and the environment, K/W
R^*_{tot} = overall thermal resistance between the molten salts and the environment without foundation, K/W
R_{tot_lat} = thermal resistance of the lateral surface of the storage tank, K/W
R_{tot_roof} = thermal resistance of storage-tank roof, K/W
R_{salt_foam} = thermal resistance of molten salts—foamglas®, K/W
s = any given month in any given year during the tank's operational lifetime
SEGS = solar electric generating systems
t = time, s
t_{ax} = tax rate, %
T_{amb} = ambient temperature, °C
T_{conc} = temperature of the reinforced concrete, 90°C
$T_{salt}(t)$ = bulk temperature of the molten salts, °C
T_{soil} = temperature of the soil in contact with the foundation, °C
TIC = total investment cost, M€
U_{fs} = overall heat coefficient between foundation and the soil, W/m^2 K
η_s = average net electric efficiency of the integrated combined solar power plant during any given month, s, with reference to collected solar power, %

References

[1] Mills, D., 2004, "Advances in Solar Thermal Electricity Technology," Sol. Energy, **76**, pp. 19–31.
[2] Schlaich, J., Bergermann, R., Schiel, W., and Weinrebe, G., 2005, "Design of Commercial Solar Updraft Tower Systems—Utilization of Solar Induced Convective Flows for Power Generation," ASME J. Sol. Energy Eng., **127**, pp. 117–124.
[3] Eck, M., and Zarza, E., 2006, "Saturated Steam Process With Direct Steam Generating Parabolic Troughs," Sol. Energy, **80**, pp. 1424–1433.
[4] Zarza, E., Rojas, M. E., Gonzalez, L., Caballero, J. M., and Rueda, F., 2006, "INDITEP: The First Pre-Commercial DSG Solar Power Plant," Sol. Energy, **80**, pp. 1270–1276.
[5] Zarza, E., Valenzuela, L., Leòn, J., Hennecke, K., Eck, M., Weyers, H.-D., and Eickhoff, M., 2004, "Direct Steam Generation in Parabolic Troughs: Final Results and Conclusions of the DISS Project," Energy, **29**, pp. 635–644.
[6] Eck, M., Zarza, E., Eickhoff, M., Rheinlander, J., and Valenzuela, L., 2003, "Applied Research Concerning the Direct Steam Generation in Parabolic Troughs," Sol. Energy, **74**, pp. 341–351.
[7] Eck, M., and Steinmann, W.-D., 2002, "Direct Steam Generation in Parabolic Troughs: First Results of the DISS Project," ASME J. Sol. Energy Eng., **124**, pp. 134–139.
[8] Zarza, E., Valenzuela, L., Leòn, J., Weyers, H.-D., Eickhoff, M., and Eck, M., 2002, "The DISS Project: Direct Steam Generation in Parabolic Trough Systems. Operation and Maintenance Experience and Update on Project Status," ASME J. Sol. Energy Eng., **124**, pp. 126–133.
[9] Dersch, J., Geyer, M., Herrmann, U., Jones, S. A., Kelly, B., Kistner, R., Ortmanns, W., Pitz-Paal, R., and Price, H., 2004, "Trough Integration Into Power Plants—A Study on the Performance and Economy of Integrated Solar Combined Cycle Systems," Energy, **29**, pp. 947–959.
[10] Herrmann, U., and Kearney, D. W., 2002, "Survey of Thermal Energy Storage for Parabolic Trough Power Plants," ASME J. Sol. Energy Eng., **124**, pp. 145–152.
[11] Laing, D., Steinmann, W. D., Tamme, R., and Richter, C., 2006, "Solid Media Thermal Storage for Parabolic Trough Power Plants," Sol. Energy, **80**, pp. 1283–1289.
[12] Kearney, D., Kelly, B., Herrmann, U., Cable, R., Pacheco, J., Mahoney, R., Price, H., Blake, D., Nava, P., and Potrovitza, N., 2004, "Engineering Aspects of a Molten Salt Heat Transfer Fluid in a Trough Solar Field," Energy, **29**, pp. 861–870.
[13] Moens, L., Blake, D. M., Rudnicki, D. L., and Hale, M. J., 2003, "Advanced Thermal Storage Fluids for Solar Parabolic Trough Systems," ASME J. Sol. Energy Eng., **125**, pp. 112–116.
[14] Michels, H., and Pitz-Paal, R., 2006, "Cascaded Latent Heat Storage for Parabolic Trough Solar Power Plants," Sol. Energy, **81**, pp. 829–837.
[15] Brosseau, D., Kelton, J. W., Ray, D., Edgar, M., Chisman, K., and Emms, B., 2005, "Testing of Thermocline Filler Materials and Molten-Salt Heat Transfer Fluids for Thermal Energy Storage Systems in Parabolic Trough Power Plants," ASME J. Sol. Energy Eng., **127**, pp. 109–116.
[16] Pacheco, J. E., Showalter, S. K., and Kolb, W. J., 2002, "Development of a Molten-Salt Thermocline Thermal Storage System for Parabolic Trough Plants," ASME J. Sol. Energy Eng., **124**, pp. 153–159.